Chapter 12
Natural Landslides Which Impact Current Regulating Services: Environmental Preconditions and Modeling

Jörg Bendix, Claudia Dislich, Andreas Huth, Bernd Huwe, Mareike Ließ, Boris Schröder, Boris Thies, Peter Vorpahl, Julia Wagemann, and Wolfgang Wilcke

12.1 Introduction

Manifold interactions between the abiotic and the biotic environment doubtlessly exist in the complex biodiversity hotspot of the Rio San Francisco valley. Hitherto, it is not unveiled how the natural forest and its biodiversity which regulates (regulating services) the local abiotic conditions (climate, water, soil) is subjected to feedbacks regarding the preservation of species richness. Different hypotheses how interactions and feedbacks between abiotic factors and biota contribute to determine biodiversity are under discussion since decades. Widely accepted in the

J. Bendix (✉) • B. Thies • J. Wagemann
Faculty of Geography, Laboratory for Climatology and Remote Sensing, University of Marburg, Deutschhausstraße 10, 35032 Marburg, Germany
e-mail: bendix@staff.uni-marburg.de

C. Dislich • A. Huth
Department of Ecological Modelling, Helmholtz Centre for Environmental Research – UFZ, P.O. Box 500 136, 04301 Leipzig, Germany

B. Huwe • M. Ließ
Department of Soil Physics, University of Bayreuth, Universitätsstraße 30, 95447 Bayreuth, Germany

B. Schröder
Department of Ecology and Ecosystem Management, Technical University of Munich, Emil-Ramann-Str 6, 85354 Freising-Weihenstephan, Germany

P. Vorpahl
Department of Ecology and Ecosystem Management, Technical University of Munich, Emil-Ramann-Str 6, 85354 Freising-Weihenstephan, Germany

Institute of Earth and Environmental Science, University of Potsdam, Karl-Liebknecht-Str. 24-25, 14476 Potsdam-Golm, Germany

W. Wilcke
Geographic Institute of the University of Bern (GIUB), University of Bern, Hallerstrasse 12, 3012 Bern, Switzerland

J. Bendix et al. (eds.), *Ecosystem Services, Biodiversity and Environmental Change in a Tropical Mountain Ecosystem of South Ecuador*, Ecological Studies 221,
DOI 10.1007/978-3-642-38137-9_12,

group of hypotheses regarding internal feedbacks controlling biodiversity is the intermediate disturbance hypothesis (IDH) (Connell 1978; Molino and Sabatier 2001) which means that moderate disturbances are fostering the highest degree of species richness. Roxburgh et al. (2004) stressed that the original specification of the IDH requires patchy disturbances. Sheil and Burslem (2003) emphasized that landslides are proven to be one important patchy disturbance type promoting biodiversity above and below ground. It is meanwhile undisputed that landslides are a major factor of natural disturbance in the mountain forest of the study area (Wilcke et al. 2003, Chap. 1). While reducing the overall aboveground biomass, landslides increase the spatial heterogeneity of biomass distribution and thus create distinct habitat types (Dislich and Huth 2012). Particularly plant succession after a landslide and the related above ground species pool of mosses, lichens, vascular plants like orchids and pioneer tree species contribute to the high biodiversity of the mountain rain forest and its resilience against natural disturbances (refer to Chap. 8). Below ground diversity and abundance (e.g., AM fungi) might be affected by landslides, too (refer to Chap. 7).

Profound knowledge on physical interactions between abiotic factors and the forest that are assumed to trigger landslides is mandatory for predicting landslide occurrence probabilities and potential future changes.

The basic factors controlling landslide occurrence in the study area are geology in terms of bedrock material, climate, and topography (Fig. 12.1).

While the geological substrate in the study area is nearly homogenous, the topographic situation is highly variable. In this context, elevation, slope position, steepness, and terrain curvature are the most important factors (Sect. 12.2.1, Fig. 12.1a). Regarding climatic parameters, particularly the abundant rainfall enhances the weight of vegetation and soil and reduces soil strength. Because rainfall generally increases with terrain altitude (Chaps. 1, 19, and 24) elevation is a good proxy for rainfall. High wind speed and resulting dynamic pressure particularly at windward sides at higher altitudes transfer the dynamic stress of trees into the tree root layer and thus are also expected to be important predictors to assess landslide risks (Sect. 12.3.3, Fig. 12.1c). Soil conditions (thickness of the organic and mineral soil layers, soil water logging conditions as indicated by stagnic horizon occurrence probability) are suspected to play a major role and should be considered for landslide prediction (Fig. 12.1b), too. Beyond physical interactions, also chemical interactions might influence the risk for landslides. The role of a specific abiotic–biotic interaction — the relation between soil nutrient availability and fine litter production as a proxy for biomass production and thus vegetation and organic layer weight (Fig. 12.1d) — is discussed in this chapter. Nutrient availability in the soil as an important control of biomass production (influencing the weight of the vegetation) and organic matter degradation (influencing the weight of organic layers) is thus assumed to be an important predictor for landslide probability.

To disentangle the processes responsible for landslide activity, spatial explicit models as presented in this chapter are necessary, which are currently based solely on topographical predictor variables (Sect. 12.2.1, Fig. 12.1a). For a future improvement of the presented model, further spatial input data of relevant climatic

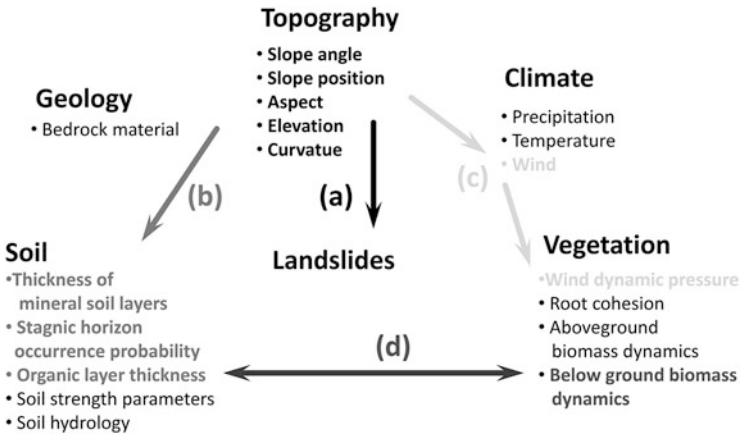

Fig. 12.1 Overview on factors controlling landslide susceptibility in the study area. *Arrows* indicate aspects covered by this chapter: The topographic control on landsliding (**a**), on soil formation (**b**), on the distribution of local wind fields (**c**), and the dependence of organic matter decomposition, organic layer mass, and biomass dynamics (**d**). Future model parameters written in *gray* are developed and discussed in this chapter

and soil predictors as described above are required (Sects. 12.2.2–12.2.4). Most of these data were not available when developing the model described in Sect. 12.2.1. Consequently, this chapter is also devoted to exemplarily present methods to regionalize point-based soil and climate data.

It should be stressed that landslides in a protected, unused pristine mountain forest are not a direct ecosystem service (refer to Chap. 4). However, natural landslide dynamics cause feedbacks to other abiotic and biotic ecosystem components which give reason to expect impacts on several service levels as, e.g., regulation services. On the landscape scale, naturally and anthropogenically induced landslides seem to play a major role in sediment regulation of the catchment, being claimed to be responsible for a quasi-continuous export of sediment loads independent on precipitation peaks (refer to Chap. 9). On the smaller scale, nutrient regulation is clearly affected by landslides. Nutrients are removed with the biomass and the organic layers from the slide area but deposited and concentrated in its foot area (refer to Chap. 11). Regarding carbon regulation, landslides are characterized by reduced tree growth on the slides due to the poor nutrient conditions, thus diminishing aboveground carbon stocks considerably (refer to Chap. 24).

12.2 Methods

12.2.1 The Statistical Landslide Model

Conditions leading to slope failure in the past are likely to cause landslides in the future as well. Thus, inventories of past landslides combined with topographic information and thematic maps of controlling factors are used to train statistical

landslide models with multiple predictors. Univariate response curves of these models can provide insights into driving factors of landslides if the following preconditions are met: (1) The model quality (in terms of performance and calibration) is sufficient. (2) Consistency between mechanistic assumptions and training data is maintained. (3) The chosen predictors are interpretable.

(1) Vorpahl et al. (2012) provided a unified framework to train, test and compare different statistical methods. Applying this framework to eight different methods from statistics and machine learning (i.e., generalized linear and additive models, multivariate adaptive regression splines, artificial neural networks, classification tree analysis, random forests, boosted regression trees, and the maximum entropy method), they generated weighted model ensembles.
(2) Vorpahl et al. (2012) maintained consistency between training data and mechanistic assumptions by using a subset of five historical landslide inventories of the RBSF provided by Stoyan (2000) and confined their analysis to landslides that occurred in an area free of anthropogenic interference (Fig. 12.2). Furthermore, they distinguished different functional units of landslides: i.e., initiation, transport, and deposition zones. This distinction is of key importance for an interpretation of univariate model response curves, since linkages between model predictors and actual mechanisms in the distinct functional units differ.
(3) In a case study, Vorpahl et al. (2012) exclusively used terrain attributes derived from a digital elevation model (DEM) as predictors: elevation above sea level (ALT), slope angle, topographic wetness index (TWI), stream power index (SPI), convergence index (CI), topographic position index (TPI) with two different radii (100 m and 500 m), and the aspect. To model landslide initiation as a phenomenon of abiotic–biotic interactions by assessing the importance of abiotic and biotic predictor values in later applications of the method, spatial parameter values as presented in the succeeding sections might be helpful.

12.2.2 Potential Model Parameter: Regionalization of Soil Data

The spatially explicit prediction of histic and stagnic soil horizons is necessary as a major precondition to understand the landslide dynamics in the study area.

Soil regionalization is based on the general concept (e.g., Jenny 1941) that soil genesis and, hence, the soils' distribution throughout the landscape mainly depend on topography, among other parameters. Therefore, topographic parameters can be used as predictors to develop digital maps of various soil attributes.

Soil horizons were assessed by 56 soil profiles and 315 auger sampling points. Key topographical parameters were calculated based on the DEM and implemented area wide as predictors in the software SAGA GIS. To collect a representative dataset, sampling sites were selected according to a 24 terrain classes comprising

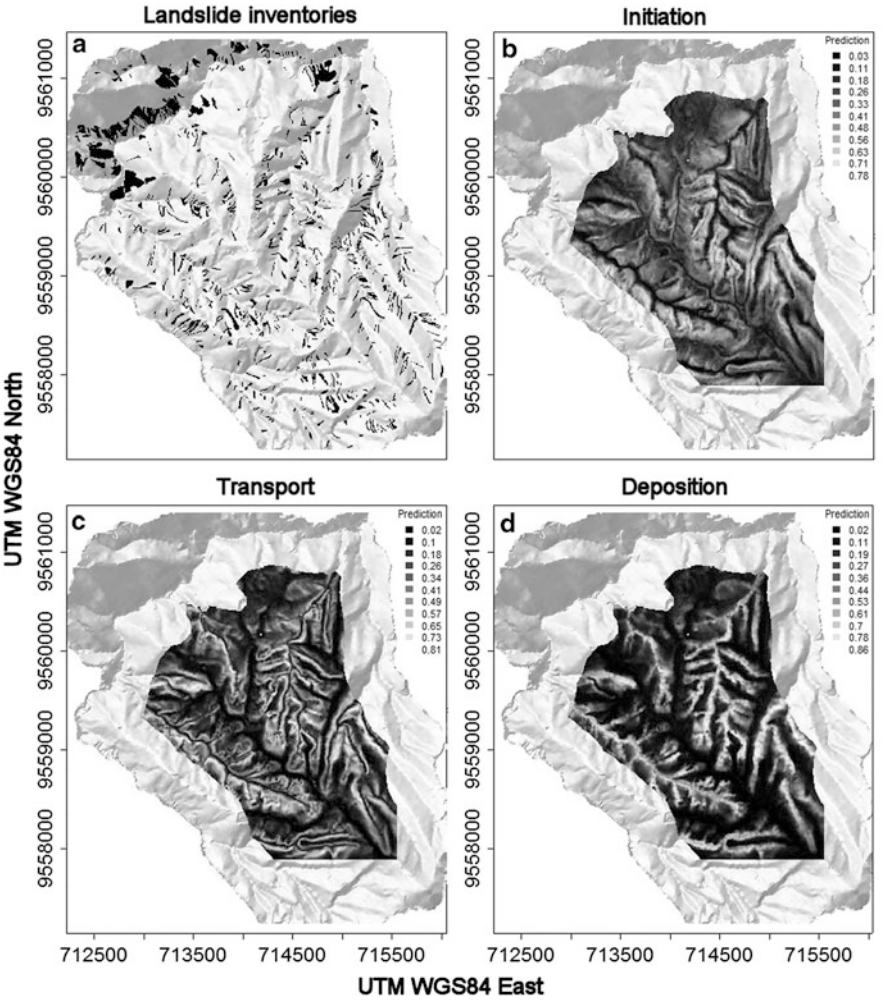

Fig. 12.2 **(a)** Landslide inventories created by evaluation of aerial photographs of five different years (i.e., 1692, 1969, 1976, 1989, and 1998) by Brenning (2005) and landslide susceptibility maps as produced by weighted model ensembles for **(b)** landslide initiation, **(c)** transport, and **(d)** deposition zones (cf. Vorpahl et al. 2012)

sampling design along transects extending along side valley slopes (Liess et al. 2009).

The regionalization as presented here is based on earlier attempts to predict these horizons (Ließ 2011). In comparison to Ließ (2011), an improvement could be achieved by focusing on (1) additional terrain parameter selection and by (2) investigating the dependence on scale as well as (3) the performance of another recursive partitioning method, Random Forest (RF) (Breiman 2001).

Table 12.1 SAGA modules to calculate terrain parameters

Terrain parameter	Module library	Module
Altitude	Terrain analysis—preprocessing	Fill sinks (Planchon/Darboux, 2001)
Slope	Terrain analysis—morphometry	Slope, aspect, curvature
Aspect		
Profile curvature		
Plan curvature		
Convergence index	Terrain analysis—morphometry	Convergence Index (search radius)
Normalized height	Terrain analysis—morphometry	Relative heights and slope positions
Valley depth		
TRI	Terrain analysis—morphometry	Terrain Ruggedness Index
Wind effect	Terrain analysis—morphometry	Wind effect
KRAarea	Terrain analysis—hydrology	Catchment area (flow tracing)
KRAslope		
SWI	Terrain analysis—hydrology	Saga Wetness Index
PISR	Terrain analysis—lighting, visibility	Potential incoming solar radiation—direct insolation

(1) Based on the investigations by Ließ (2011), predictors representing climate (altitude, PISR), water accumulation (curvature, convergence, KRAarea), water discharge (slope, KRAslope), the insulating effect of the heterogeneous geomorphology with the ridge—side valley structure in particular (TRI, normalized height, valley depth) and the wind effect (wind effect, aspect) were selected to model the soil pattern of this area, all calculated by using SAGA GIS (Table 12.1, Böhner et al. 2006).

(2) According to the assumptions of Ließ (2011) that the influence of certain predictors on soil property development is scale dependent, Brown et al. (2004) had reported this for the influence of curvature on soil texture, terrain parameters were calculated for three different GIS raster grid cell sizes (10, 20, 30 m).

(3) Because RF shows a strong dependence on the used dataset used for model development (Ließ et al. 2012), i.e., the terrain parameters used as predictors with the soil parameter as response variable, 100-fold RF calculations of the spatial water stagnation pattern as well as organic layer and stagnic horizon thickness were carried out. For each of the 100 model runs, the used dataset was varied by using 9/10 random Jackknife partitions data subsets of the complete dataset. The 100 models' prediction results were then averaged and displayed as two maps: the mean prediction value of the particular soil parameter and its prediction uncertainty which is represented by the coefficient of variation. Cross validation is applied to the remaining 1/10 of the dataset, which was not used to develop the RF models, for model evaluation.

12.2.3 Potential Model Parameter: Regionalization of Wind Data

Regionalization of meteorological point observations facilitates the analysis of interactions between the abiotic environment and biosphere (e.g., Fries et al. 2009, 2012). Strong wind pressure to forest trees might be one reason fostering landslides and shaping the tree line. Therefore, digital wind speed and dynamic pressure maps are determined using the following procedure: (1) Statistical analysis of wind speed observations using the Weibull density function. (2) Calculation of digital wind speed maps by applying a sheltering factor—algorithm to a DEM. (3) Validation of calculated wind speed using model-independent meteorological stations. (4) Calculation of dynamic pressure maps based on the tropical standard atmosphere and the generated wind speed maps.

(1) Point measurements of hourly wind speed data and the wind direction at 2 m above surface level for a period of 8 years (1999–2006) for five meteorological stations (Cerro, ECSF, El Trio, Paramo, TS1, Fig. 12.3) were analyzed regarding mean and maximum wind speed. According to meteorological conventions (e.g., Weisser 2003), mean and maximum wind speed per 45°-wind direction class are derived from the Weibull density function (50 % and 95 % percentile), where the parameters of the distribution are estimated by the maximum likelihood method.
(2) Wind speed maps are calculated in three steps: First, data of the station Zamora and the highest meteorological station (Paramo) are used to calculate a linear decrease of average and maximum background wind speed with decreasing terrain altitude. Second, the approach of Winstral and Marks (2002) is used to derive the maximum upwind slope parameter which is a measure of topographic shelter or exposure relative to a particular wind direction. The finally determined shelter factor is multiplied with the background wind speed for every pixel, providing the digital wind speed maps for every wind direction class.
(3) Wind speed is extracted for the grid points of the meteorological stations not used for the regionalization and compared to the modeled data. For the most stations (e.g., ECSF, Cerro), the correlation is significant and well-suited, except for the station El Tiro which is known to be strongly influenced by topographic venturi effects not considered by the regionalization method.
(4) Finally maps of average and maximum dynamic pressure are calculated from the wind speed maps and average air density where the latter is derived by blending the tropical standard atmosphere with the DEM.

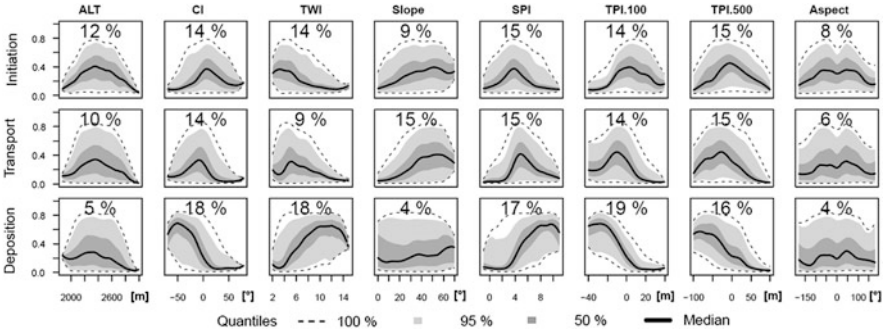

Fig. 12.3 Univariate response curves (*black lines*) and predictor importance scores of weighted ensembles of statistical models. Response quartile ranges are shaded in *gray*. The *curves* in each column show the probability of observing a landslide initiation, transport or deposition zone as a function of a single predictor variable, i.e., elevation above sea level (ALT), the convergence index (CI), indicating small scale concavities (CI < 0) or convexities (CI > 0), the topographic wetness index (TWI), the slope angle (Slope), the stream power index (SPI), the topographic position index (TPI), describing the difference between local elevation and the mean elevation within two different radii of 100 m (TPI.100) and 500 m (TPI.500), respectively, and the direction of the steepest slope angle (Aspect) (Vorpahl et al. 2012)

12.2.4 Soil Properties and Litterfall

Between 1998 and 2010 we collected data from 12 sites in the study area (one in each of the microcatchments (MC) 1 and 3, three in each of MCs 3 and 5 and the four control sites of Nutrient Manipulation Experiment (NUMEX, for locations see Chap. 1, NUMEX is explained in Chap. 23). Monitoring in MC2 lasted for 12 years, in MCs 1, 3, and 5 for 5 years and in NUMEX for 1 year. At each site, mass of organic layer was determined once by measuring depth and densities of the organic horizons (Oi, Oe, and Oa) and mass of fine litterfall was determined with three- to sixfold replicated 0.3×0.3 m^2 to 0.6×0.6 m^2 large litter traps in at least monthly resolution. Furthermore, free-draining litter lysimeters just below the organic layer were used to collect litter leachate in weekly to fortnightly resolution in which mineral N (NH_4^+–N + NO_3^-–N) concentrations were determined with a Continuous Flow Analyzer and K, Na, Ca, and Mg concentrations with flame Atomic Absorption Spectrometry.

12.3 Results and Discussion

12.3.1 Statistical Landslide Modeling

With the exception of classification tree analysis all techniques performed comparatively well while being outperformed by weighted model ensembles (refer to Vorpahl et al. 2012 for details). As expected, models trained on different functional units of landslides led to different model outcomes (Fig. 12.2).

Univariate model response curves to changes in predictor values—also called partial dependency plots (Fig. 12.3)—show that landslide deposition zones tend to be located at valley bottoms, indicated by high values of SPI and TWI as well as by negative values of CI and TPI.

Landslides follow the local topography by sliding along shallow ducts in the slope as indicated by a maximum susceptibility for transport zones at slightly negative values of CI and TPI. The response curve for initiation zones to changes in slope indicated an increasing contribution up to ~52°. Even steeper slopes lead to a decrease of landslide susceptibility. This can be attributed to the fact that on extremely steep slopes the soil layer is usually thinner and hence insufficient for landslide initiation.

Model response to elevation above sea level exposed an increasing landslide initiation probability with elevation up to 2,400 m a.s.l. At higher elevations, landslide initiation probability decreases. Rollenbeck (2006) reported an altitudinal increase of average precipitation (from about 2,050 mm a^{-1} at 1,960 m a.s.l. up to 4,400 mm a^{-1} at 3,200 m a.s.l.) in the research area. If rainfall is an important factor, this should hint towards a positive correlation between precipitation and landslide susceptibility which contradicts the above finding. As additional factors at the intersection from dense forest into the Páramo, lower standing biomass and lower inclination may strongly reduce landslide formation. Furthermore, Bussmann et al. (2008) gave a possible explanation for the decreasing landslide susceptibility at higher elevations by a change in soil substrate from slightly metamorphosed clayey/sandy sediments, originating from phyllites, at the lower and intermediate elevations to a more quartzite rich substrate at higher elevations.

Other altitudinal gradients reported for the research area are related to vegetation. The decrease of average tree heights with higher elevations (Bräuning et al. 2008), for example, may cause a reduced contribution of plant biomass to slope instability. Smaller trees are less capable of transferring wind forces into the ground via a turning moment. Soethe et al. (2006a, b) as well as Leuschner et al. (2007) reported an altitudinal change in tree root structure and in the ratio of aboveground to belowground biomass. Thus an increase of root contribution to slope stability at higher elevations can be additionally suspected.

12.3.2 Digital Soil Maps

To predict organic layer thickness, the models based on 20 or 30 m DEM resolution performed better than those using 10 m. Regarding the prediction of the occurrence of a stagnic color pattern, all models using 10 m resolution performed better or equally well than those of lower resolution. Chaplot et al. (2000) found prediction accuracy to be highly dependent on DEM resolution: Regarding the prediction of hydromorphic features 10 m DEM resolution outperformed lower resolutions. Compared to the median r_{xy} resulting from CART methodology and a smaller number of prediction parameters (Ließ 2011), model performance was now

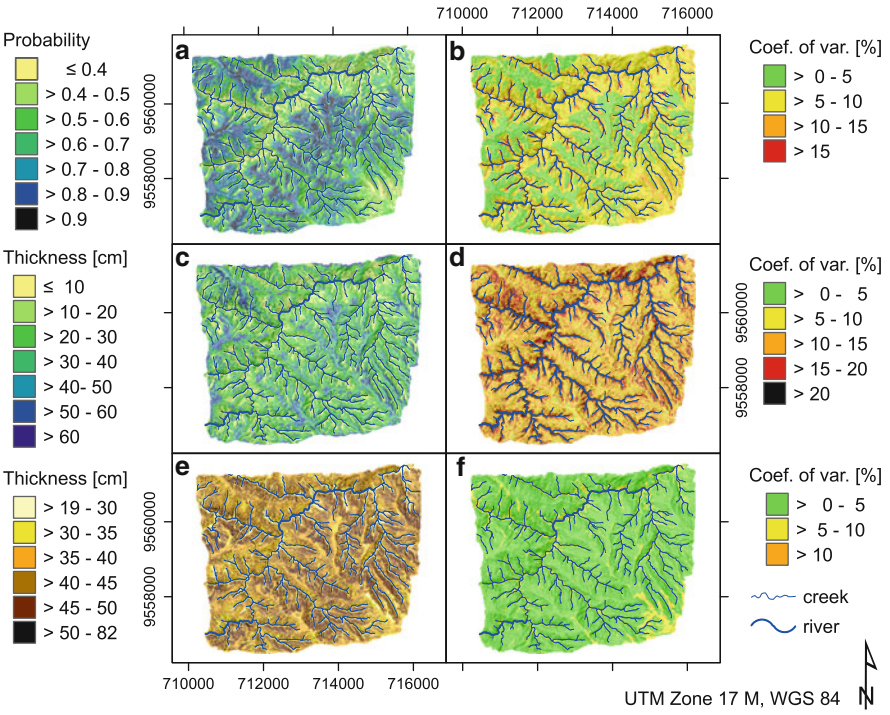

Fig. 12.4 Mean stagnic horizon occurrence probability (**a**) and thickness (**c**) with coefficient of variation (**b**, **d**) and mean organic layer thickness (**e**) with coefficient of variation (**f**) (Overlaid hill shading with light source from north)

improved for all three predicted soil parameters: regarding stagnic horizon occurrence probability it was improved by 0.1 (0.6), regarding horizon thickness it was doubled (0.36), and regarding organic layer thickness it was more than doubled (0.47).

The digital soil map of the stagnic horizon occurrence probability is shown in Fig. 12.4a, b. A low coefficient of variation ($\leq$10 % for $>$80 % of the area, see Fig. 12.4b) shows that the dataset is well suited to model the stagnic properties pattern within this area. The influence of the relative slope position on the occurrence probability is clearly visible: The exposed mountain ridges between 2,100 and 2,650 m a.s.l. display a very high probability of stagnic soil properties, $>$0.8, which is decreasing down the side valley slopes to a probability of $\leq$0.4 (minimum = 0.2). The flat platform-like areas on top of the ridges, display a particularly high probability of $>$0.9. The areas below 2,100 and above 2,650 m a.s.l. are predicted with an overall lower probability. Below 2,100 m a.s.l. the lower bulk density (Ließ et al. 2011) and above 2,650 m a.s.l. the coarser soil texture (Ließ et al. 2012) leads to a higher saturated hydraulic conductivity and therefore less chance for the development of stagnic soil properties. For the development of the model to predict stagnic horizon occurrence probability, all terrain parameters were included.

This confirms the assumption that it is the complex pattern of climate (altitude, PISR), water accumulation (curvature, convergence, KRAarea), water discharge (slope, KRAslope), the insulating effect of the heterogeneous geomorphology with the ridge—side valley structure in particular (TRI, normalized height, valley depth) as well as the wind effect (wind effect, aspect) which lead to the distribution pattern of stagnic soil properties within the investigation area.

The model to regionalize stagnic horizon thickness is less stable than the model to predict the horizon's occurrence probability. This is indicated by the higher values of the coefficient of variation in Fig. 12.4d. Ließ (2011) describes similar results. According to Park and Vlek (2002), soil attributes of which the vertical distribution is strongly determined by pedogenesis or unknown factors are poorly modeled by environmental variables. Accordingly, the frequent change of parent material within one soil profile (Ließ et al. 2012) might be the reason why stagnic horizon thickness cannot be explained by geomorphology alone. The thickest stagnic layers >40 or even >60 cm are found along the mountain ridges, with decreasing thickness while proceeding down side valley slopes.

The low uncertainty of the digital soil map of the organic layer (Fig. 12.4e, f) indicates a stable model. The thickest organic layers are found on mid-slope positions, decreasing towards the creeks and towards the crests. Furthermore, altitude is not among the five most influential predictors of organic layer thickness and there is no correlation between the occurrence of stagnic horizons and organic layer thickness. This is unexpected because in previous work it was shown that the crests had usually thicker organic layers than the valley bottom positions in the study area (Wilcke et al. 2010) in line with reports from a similar forest in Puerto Rico (Silver 1994). Furthermore, studies in Costa Rica (Marrs et al. 1988; Grieve et al. 1990) and at our study site in Ecuador (Schrumpf et al. 2001; Wilcke et al. 2008a, b) have shown that organic layer thickness usually increases with increasing altitude because of decreasing microbial turnover of organic matter with increasing altitude (Benner et al. 2010). Table 10.1 shows a general trend towards increasing organic layer thickness with altitude. However, the transect that was investigated covers a much larger distance (30 km compared to c. 4 km), and spatial data coverage is therefore limited. Taking a closer look, the results of Chap. 10 also do not describe any positive correlation between organic layer thickness and altitude for the altitudinal range between 1,890 and 3,060 m a.s.l. studied here. Finally, it is assumed that soil waterlogging limits organic matter turnover (Schuur and Matson 2001; Roman et al. 2010) which results in the expectation of a positive correlation between the occurrence of waterlogging (as indicated by stagnic horizons) and organic layer thickness. However, there is a considerable variation in organic layer thickness at small scale (Wilcke et al. 2002, 2008b) illustrating that none of altitude, topographic position, and waterlogging alone can explain the entire variability in organic layer thickness.

A possible explanation for the seeming contradictions might be that our dataset is representative for the whole study area and therefore also includes landslide sites with incomplete organic layers which form an important part of the studied forest area (Bussmann et al. 2008). Wilcke et al. (2003) have shown that the full

regeneration of the organic layer only occurs at the time scale of a few decades. It also seems likely that waterlogging favors the initiation of landslides because of the associated high soil weight (Ließ et al. 2011). The results in the literature, in contrast, usually refer to undisturbed old-growth forest sites. An alternative explanation might be that litterfall rates are lower on crest sites than at lower topographic positions associated with a smaller accumulation of organic matter on top of the mineral soil. However, in Sect. 12.3.4 we show for a limited dataset of 12 study sites that the decrease in litterfall rates is overcompensated by the decrease in degradation rates resulting in even higher organic layer thickness at low litterfall rates. We conclude that the relationships of altitude, topographic position, and waterlogging with organic layer thickness might have to consider the state of succession after landslide to explain and predict the spatial distribution of organic layer thickness in the study area.

12.3.3 Digital Wind Maps

Figure 12.6a shows the calculated digital map of maximum wind speed which reveals spatial structures comparable to the map of mean wind speed (not shown here). Maximum wind speed increases with altitude but is locally modified by topographic shelter effects towards the predominant wind direction. Obviously, steep and narrow valleys and ravines breaching the Cordillera exhibit the lowest wind speeds (partly close to calm) on a specific altitudinal level. It is striking that especially the east-facing slopes without any protection by upstream topographic structures exhibit severe wind speeds up to 17 m s^{-1}. The reason is the all-year dominating circulation from the east (Rollenbeck and Bendix 2011) impinging particularly the eastern slopes of the Cordillera. The high wind speeds at relatively low altitudes are a result of the Andean depression (Chap. 1) which allows the easterlies to affect the upper mountain areas nearly unbridled. By blending the land use classification of Göttlicher et al. (2009) with the digital maps of mean and maximum dynamic pressure, the interaction of wind pressure and trees can be assessed, e.g., for the tree line ecotone (Fig. 12.5b). The statistical evaluation clearly reveals that the trees at the treeline of the eastern escarpment exhibit clearly stronger mechanical exposure than on the western slopes where in the most situations, wind dynamic pressure falls into the lowest category (mean < 5 N m^{-2}; maximum < 20 N m^{-2}).

12.3.4 Chemical Interactions: Soil Nutrients and Litter

There were close positive correlations between nutrient concentrations in soil solution and annual fine litterfall as proxy of biomass productivity and close negative correlations between nutrient concentrations in soil solution and mass of

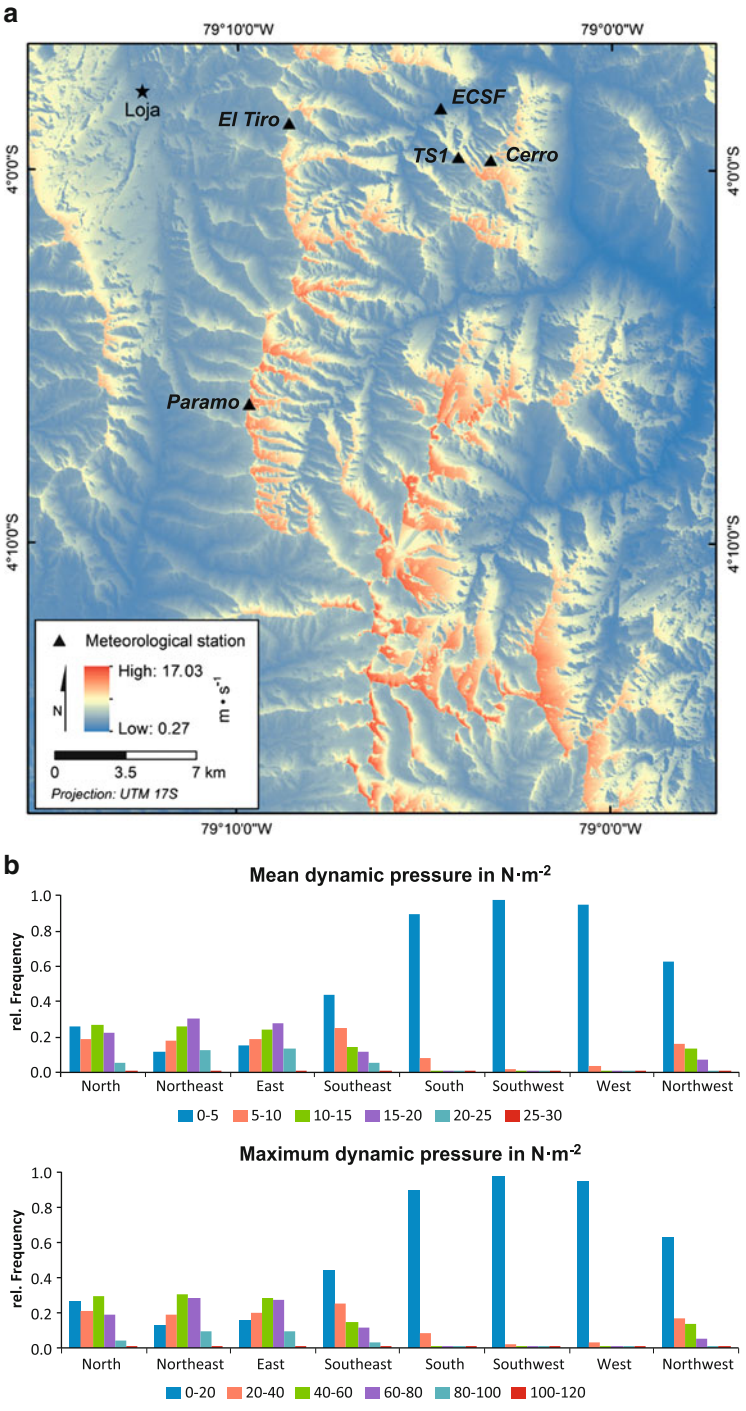

Fig. 12.5 (**a**) Digital map of maximum wind speed [95 % percentile] determined as an occurrence-weighted average of eight wind direction classes. (**b**) Mean and maximum dynamic pressure depending on aspect along the tree line ecotone

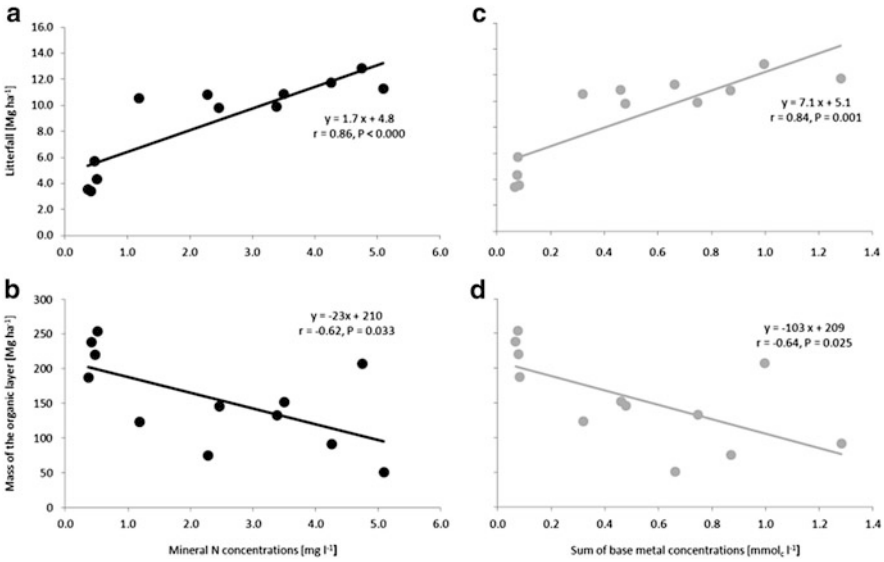

Fig. 12.6 Relationship between mean mineral N concentrations (NH_4^+–N + NO_3^-–N) in litter leachate and (**a**) mean annual litterfall and (**b**) mass of the organic layer and between mean sum of base metal concentrations (charge equivalents of K, Na, Ca, and Mg) in litter leachate and (**c**) mean annual litterfall and (**d**) mass of the organic layer. Mean nutrient concentrations in litter leachate and mean annual litterfall was determined during 1–10 years depending on the specific site

organic layer (Fig. 12.6). The effect of bases (K, Na, Ca, and Mg) is more pronounced than that of N. Consequently, increased nutrient availability resulted in increased fine litterfall production and—if litterfall is proportional to standing biomass—increased weight of vegetation. The increased weight of vegetation is counteracted by decreased weight of organic layer because of a faster turnover at higher nutrient availability. Expressed in percent of the intercept the response of litterfall is more pronounced (35 % for N and 139 % for bases) than that of mass of organic layer (−11 and −49 %) suggesting that the standing biomass will more strongly increase than the mass of the organic layer decrease if nutrient availability improves. The latter can be expected for the near future because of increased dryness enhancing release of nutrients from the organic matter by mineralization and because of rising deposition of reactive nitrogen and possibly also of base metals because of the shortening of the El Niño Southern Oscillation (ENSO) cycle (see Chap. 11). This might imply that the total weight of vegetation plus organic layer will increase in the near future in response to environmental change thereby enhancing the risk of landslides.

Nutrient availability in the study area generally decreases with increasing altitude and at the same altitude is different between valley bottom and ridge top position (Wilcke et al. 2008b, 2010). Furthermore, the frequently occurring shallow landslides in the study area remove the vegetation and the organic layer resulting in nutrient loss which is only replenished during a few decades (Wilcke et al. 2003).

The latter effect is not included in the relationship between nutrient availability and litterfall/mass of organic layer in Fig. 12.6 because all our measurements were taken at old-growth forest sites which were not impacted by landslides in the last decades. The high variability of altitude and topography in our study area results in a high spatial variability of nutrient availability and thus also a high ability of organic layer mass and standing forest biomass together determining the weight on top of the mineral soil (Wilcke et al. 2002; Moser et al. 2008).

12.4 Conclusion

The presented statistical model ensembles revealed that the occurrence of landslides is mainly controlled by factors related to the general position along a slope (i.e., ridge, open slope, or valley). However, there is a clear contradiction between the altitudinal gradient of rainfall (increasing with altitude) as an assumed major trigger and landslide probability (decreasing with altitude above 2,400 m a.s.l.). This indicates that more complex interactions control landslide activity in the study area which can be explained with a model ensemble purely forced with DEM-derived proxy predictors. Digital soil maps show a sandier soil texture and lower soil water logging probability above 2,400 m a.s.l and hence provide a good explanation. We further assume that variation in above and belowground biomass mitigating dynamic wind pressure to the forest in the higher parts are major factors causing these contradictory findings. Thus, it is necessary to provide further spatial predictor maps related to geology, vegetation biomass, and climate. By additionally considering predictors related to vegetation, soil and climate, statistical models will allow for predicting potential future changes in landslide probability patterns. Dynamic forest models like FORMIND can be used to further quantify effects on the aboveground biomass production (Chap. 24).

Regarding maps of soil conditions, statistical models based on comprehensive soil field surveys are applied to spatially predict organic layer and stagnic horizon thickness as well as stagnic horizon occurrence probability. Forcing parameters are solely derived from topographical analyses of the DEM. Even if the main influence of the relative slope position as exposed mountain ridges and flat platform-like areas on top of the ridges are the best predictors for the occurrence probability of stagnic horizons, the results point out complex interactions of different factors behind this. Particularly, the determination of the stagnic horizon thickness is less stable, most likely due to unconsidered, non geomorphologic factors. For prediction of organic layer thickness, the degree of succession after landslide might also play an important role and should be considered besides the well established relationship of waterlogging, topographic position, and altitude with organic layer thickness.

Digital maps of mean and maximum wind speeds as well as dynamic wind pressures as additional potential forcing parameters were derived by means of field observations of wind speed, data on air density, and a DEM by introducing a terrain shelter factor. It could be shown that dynamic pressure to the forest generally

increases with altitude but differs with exposition to the main wind direction. Because easterly wind directions are predominant, the tree line ecotone on the eastern slopes is affected by clearly higher wind stress.

Finally, it could be shown that interactions in the biogeochemical cycles might be relevant for the risk of landslides. Nutrient availability in soil influenced litterfall production positively and organic layer thickness negatively. An increased nutrient availability in the future will most likely result in an increase of standing biomass, thus, enhancing the risk of landslides in response to future environmental change.

Regarding ecosystem services, landslide dynamics will influence different service levels. As emphasized in the introduction, landslides are most likely a precondition for the high biological diversity in the mountain forest and thus, directly related to the cultural services of the forest (Chap. 4). Because the forest structure characterized by its high species richness properly regulates abiotic processes, landslides indirectly contribute to the regulating services of the forest (Chap. 4) too. On the scale of a single landslide, regulation of abiotic parameters changes significantly. For instance, microclimate (temperature, humidity) regulation is reduced in comparison to areas sheltered by tree canopies (Fries et al. 2009, 2012; Chap. 9). On this scale also sediment and nutrient regulation are affected. While sediment and its nutrient is accumulated at the forest edges on the foot of the slide, also slope wash of matter is higher in young landslides than under natural forest (e.g., Larsen et al. 1999). On the scale of the forest as a mosaic of trees and gap areas originating, e.g., from landslides, mass and energy fluxes to the atmosphere are different than those of closed canopies (e.g., Zhang et al. 2007) which means that landslides maintain the specific regulation of forest–atmosphere interactions. Also the carbon regulation function of the mountain ecosystem is determined by the landslide occurrence. Landslides increase carbon turnover and change the forest composition towards a higher fraction of pioneer species—however overall forest productivity may be reduced compared to old growth forest without landslide disturbances due to the unfavourable environmental conditions on landslide sites (Chap. 24).

References

Benner J, Vitousek PM, Ostertag R (2010) Nutrient cycling and nutrient limitation in torpical montane cloud forests. In: Bruijnzeel LA, Scatena FN, Hamilton LS (eds) Tropical montane cloud forests. International hydrology series. Cambridge University Press, Cambridge, pp 90–100

Böhner J, McCloy KR, Strobl J (2006) SAGA – analysis and modelling application. Göttinger Geographische Abhandlungen, vol 115. Geographisches Institut der Universität Göttingen

Bräuning A, Homeier J, Cueva E, Beck E, Günter S (2008) Growth dynamics of trees in tropical mountain ecosystems. In: Beck E, Bendix J, Kottke I, Makeschin F, Mosandl R (eds) Gradients in a tropical mountain ecosystem of Ecuador (Ecological Studies 198). Springer, Berlin, pp 291–302

Breiman L (2001) Random forests. Machine Learning 45:5–32

Brenning A (2005) Spatial prediction models for landslide hazards: review, comparison and evaluation. Nat Hazards Earth Syst Sci 5:853–862

Brown DJ, Clayton MK, McSweeney K (2004) Potential terrain controls on soil color, texture contrast and grain-size deposition for the original catena landscape in Uganda. Geoderma 122:51–72

Bussmann RW, Wilcke W, Richter M (2008) Landslides as important disturbance regimes causes and regeneration. In: Beck E, Bendix J, Kottke I, Makeschin F, Mosandl R (eds) Gradients in a tropical mountain ecosystem of Ecuador. Ecological studies, vol 198. Springer, Berlin, pp 319–330

Chaplot V, Walter C, Curmi P (2000) Improving soil hydromorphy prediction according to DEM resolution and available pedological data. Geoderma 97:405–422

Connell JH (1978) Diversity in tropical rain forests and coral reefs. Science 199:1302–1310

Dislich C, Huth A (2012) Modelling the impact of shallow landslides on forest structure in tropical montane forests. Ecol Model 239:40–53

Fries A, Rollenbeck R, Göttlicher D, Nauß T, Homeier J, Peters T, Bendix J (2009) Thermal structure of a megadiverse Andean mountain ecosystem in southern Ecuador, and its regionalization. Erdkunde 63:321–335

Fries A, Rollenbeck R, Nauß T, Peters T, Bendix J (2012) Near surface air humidity in a megadiverse Andean mountain ecosystem of southern Ecuador and its regionalization. Agric For Meteorol 152:17–30

Göttlicher D, Obregón A, Homeier J, Rollenbeck R, Nauß T, Bendix J (2009) Land cover classification in the Andes of southern Ecuador using Landsat ETM+ data as a basis for SVAT modelling. Int J Remote Sens 30:1867–1886

Grieve IC, Proctor J, Cousins SA (1990) Soil variation with altitude on volcan Barva, Costa Rica. Catena 17:525–534

Jenny H (1941) Factors of soil formation. A system of quantitative pedology. Dover, New York

Larsen MC, Torres-Sánchez AJ, Concepción IM (1999) Slopewash, surface runoff and fine-litter transport in forest and landslide scars in humid-tropical steeplands, Luquillo Experimental Forest, Puerto Rico. Earth Surf Process Landforms 24:481–502

Leuschner C, Moser G, Bertsch C, Röderstein M, Hertel D (2007) Large altitudinal increase in tree root/shoot ratio in tropical mountain forests of Ecuador. Basic Appl Ecol 219–230

Ließ M (2011) Soil-landscape modelling in an Andean mountain forest region in southern Ecuador. PhD Thesis, University of Bayreuth, Bayreuth

Liess M, Glaser B, Huwe B (2009) Digital soil mapping in southern Ecuador. Erdkunde 63:309–319

Ließ M, Glaser B, Huwe B (2011) Functional soil-landscape modelling to estimate slope stability in a steep Andean mountain forest region. Geomorphology 132(3–4):287–299

Ließ M, Glaser B, Huwe B (2012) Uncertainty in the spatial prediction of soil texture – comparison of regression tree and random forest models. Geoderma 170:70–79

Marrs RH, Proctor J, Heaney A, Mountford MD (1988) Changes in soil nitrogen-mineralization and nitrification along an altitudinal transect in tropical rain forest in Costa Rica. J Ecol 76:466–482

Molino JF, Sabatier D (2001) Tree diversity in tropical rain forests: a validation of the intermediate disturbance hypothesis. Science 294:1702–1704

Moser G, Röderstein M, Soethe N, Hertel D, Leuschner C (2008) Altitudinal changes in stand structure and biomass allocaton of tropical mountain forests in relation to microclimate and soil chemistry. In: Beck E, Bendix J, Kottke I, Makeschin F, Mosandl R (eds) Gradients in a tropical mountain ecosystem of Ecuador. Ecological studies, vol 198. Springer, Berlin, pp 229–242

Park SJ, Vlek PLG (2002) Environmental correlation of three-dimensional soil spatial variability: a comparison of three adaptive techniques. Geoderma 109:117–140

Rollenbeck R (2006) Variability of precipitation in the Reserva Biologica San Francisco/Southern Ecuador. Lyonia 9:43–51

Rollenbeck R, Bendix J (2011) Rainfall distribution in the Andes of southern Ecuador derived from blending weather radar data and meteorological field observations. Atmos Res 99:277–289

Roman L, Scatena FN, Bruijnzeel LA (2010) Global and local variations in tropical montane cloud forest soils. In: Bruijnzeel LA, Scatena FN, Hamilton LS (eds) Tropical montane cloud forests. International hydrology series. Cambridge University Press, Cambridge, pp 77–89

Roxburgh SH, Shea K, Wilson B (2004) The intermediate disturbance hypothesis: patch dynamics and mechanisms of species coexistence. Ecology 85:359–371

Schrumpf M, Guggenberger G, Schubert C, Valarezo C, Zech W (2001) Tropical montane rain forest soils: development and nutrient status along an altitudinal gradient in the south Ecuadorian Andes. Die Erde 132:43–59

Schuur EAG, Matson PA (2001) Net primary productivity and nutrient cycling across a mesic to wet precipitation gradient in Hawaiian montane forest. Oecologia 128:431–442

Sheil D, Burslem DFRP (2003) Disturbing hypotheses in tropical forests. Trends Ecol Evol 18:18–26

Silver WL (1994) Is nutrient availability related to plant nutrient use in humid tropical forests? Oecologia 98:336–343

Soethe N, Lehmann J, Engels C (2006a) Root morphology and anchorage of six native tree species from a tropical montane forest and an elefin forest in Ecuador. Plant Soil 279:173–185

Soethe N, Lehmann J, Engels C (2006b) The vertical pattern of rooting and nutrient uptake at different altitudes of a south Ecuadorian montane forest. Plant Soil 286:287–299

Stoyan R (2000) Aktivität, Ursachen und Klassifikation der Rutschungen in San Francisco/Südecuador. Diploma Thesis, Friedrich-Alexander-Unversität Erlangen-Nürnberg

Vorpahl P, Elsenbeer H, Märker M, Schröder B (2012) How can statistical models help to determine driving factors of landslides? Ecol Model 239:27–39. doi:10.1016/j.ecolmodel.2011.12.007

Weisser D (2003) A wind energy analysis of Grenada: an estimation using the 'Weibull' density function. Renew Energy 28:1803–1812

Wilcke W, Yasin S, Abramowski U, Valarezo C, Zech W (2002) Nutrient storage and turnover in organic layers under tropical montane rainforest in Ecuador. Eur J Soil Sci 53:15–27

Wilcke W, Valladarez H, Stoyan R, Yasin S, Valarezo C, Zech W (2003) Soil properties on a chronosequence of landslides in montane rain forest, Ecuador. Catena 53:79–95

Wilcke W, Oelmann Y, Schmitt A, Valarezo C, Zech W, Homeier J (2008a) Soil properties and tree growth along an altitudinal transect in Ecuadorian tropical montane forest. J Plant Nutr Soil Sci 171:220–230

Wilcke W, Yasin S, Schmitt A, Valarezo C, Zech W (2008b) Soils along the altitudinal transect and in catchments. In: Beck E, Bendix J, Kottke I, Makeschin F, Mosandl R (eds) Gradients in a tropical mountain ecosystem of Ecuador. Ecological studies, vol 198. Springer, Berlin, pp 75–85

Wilcke W, Boy J, Goller R, Fleischbein K, Valarezo C, Zech W (2010) Effect of topography on soil fertility and water flow in an Ecaudorian lower montane forest. In: Bruijnzeel LA, Scatena FN, Hamilton LS (eds) Tropical montane cloud Forests, International hydrology series. Cambridge Academic Press, Cambridge, pp 402–409

Winstral A, Marks D (2002) Simulating wind fields and snow redistribution using terrain based parameters to model snow accumulation and melt over a semi-arid mountain catchment. Hydrol Process 16:3585–3603

Zhang G, Thomas C, Leclerc MY, Karipot A, Gholz HL, Binford M, Foken T (2007) On the effect of clearcuts on turbulence structure above a forest canopy. Theor Appl Climatol 88:133–137